Improving the emission quantum yield in dinuclear Eu(III) and Tb(III) complexes with 2-fluorobenzoate.

Ànnia Tubau,[a,b] Laura Rodríguez,[a,b] Ariadna Lázaro,[a,b] Ramon Vicente,[*a.b] and Mercè Font-Bardía,[c]

Abstract

The reaction of $Ln(NO_3)_2 \cdot 6H_2O$ salts (Ln = Eu and Tb) with an excess of 2-fluorobenzoic acid (H-2FBz) in ethanol/water mixture allows the isolation of dinuclear compounds of formula $[Ln_2(\mu_2\text{-}2FBz)_4(2FBz)_2(H\text{-}2FBz)_2(H_2O)_2]$ (Ln = Eu (**1**) and Tb (**2**), 2FBz = 2-fluorobenzoate). The solid-state photoluminescence study of the complexes **1** and **2** shows the 4*f*-4*f* lanthanide transitions in the visible range with improved emission quantum yields**.** **1** and **2** are water soluble and the photoluminescence study has been also made in water and D_2O solutions, showing that the emission due to the 4*f*-4*f* electronic transitions is still present. The magnetic behavior of **1** and **2** is also reported.

[a]Departament de Química Inorgànica i Orgànica, Secció de Química Inorgànica, Universitat de Barcelona, Martí i Franquès 1-11, 08028 Barcelona, Spain. E-mail: rvicente@ub.edu
[b] Institut de Nanociència i Nanotecnologia (IN2UB). Universitat de Barcelona, 08028 Barcelona, Spain
[c]Departament de Mineralogia, Cristallografia i Dipòsits Minerals and Unitat de Difracció de R-X. Centre Científic i Tecnològic de la Universitat de Barcelona (CCiTUB). Universitat de Barcelona. Solé i Sabarís 1-3. 08028 Barcelona, Spain
Electronic supplementary information (ESI) available: CCDC 2097703 (**1**). Tables S1-S2. Figures S1-S6. For ESI and crystallographic data in CIF or other electronic format see DOI: …

Introduction

Usually lanthanide(III) (Ln(III)) coordination compounds show luminescence from 4*f*–4*f* electronic transitions within the closed shell of individual ions (responsible for the light emission). The energy bands generated from these transitions are narrow and characteristic for each Ln(III) and the emitting excited states are long-lived. Since the *f*–*f* transitions are parity-forbidden, free Ln(III) ions have extremely low molar extinction coefficients (ε_λ) for direct excitation leading to low luminescence intensity. To overcome this problem, the presence of light-harvesting ligands coordinated to the Ln(III) can enhance the metal luminescence via an energy transfer process, commonly known as antenna effect.[1-3] On the other hand, luminescent lanthanide complexes are of interest due to their wide range of applications in materials and biosciences.[1-14]

For the synthesis of Ln(III) coordination compounds, the R-benzoate anions have been widely used as ligands due to the strong interaction between the Ln(III) ions and the oxygen atoms from the carboxylate group and also because the luminescence properties generated from the strong absorbing chromophore group of the organic fragment.[1,15,16]

Recently, S. Bräse et al. have published a thorough study of lanthanide fluorobenzoates coordination compounds searching for the optimal lanthanide and optimal ligand fluorination degree to obtain photo stable, non-toxic and luminescent compounds suitable for their use as bio-probes.[17] As a conclusion of the study, the europium 2-fluorobenzoate (2FBz) dihydrate of formula $[Eu_2(2FBz)_6(H_2O)_4]$ combined the best properties with a polycrystalline quantum yield (QY) of 15%.

The quenching of the luminescence is due to high-energy vibrations (namely OH stretch for water).[1,3] In Eu(III) the gap between the $^5D_0$ and the $^7F_6$ states is approximately 12 000 cm^{-1}. It follows that the quenching of the emissive state is easily accomplished through three vibrational quanta of the O-H bond,with a vibrational energy of 3600 cm^{-1}.[1b] Taking into account the experience of our research group in the syntheses and luminescence study of 2-fluorobenzoate lanthanide(III) coordination compounds[18-19] we have considered to prepare a new europium 2-fluorobenzoate monohydrate compound of formula $[Eu_2(\mu_2\text{-}2FBz)_4(2FBz)_2(H\text{-}2FBz)_2(H_2O)_2]$ (H-2FBz is 2-fluorobenzoic acid) with the aim to increase the emission quantum yield taking into account that the number of quenching water molecules in the new compound is a half with respect to $[Eu_2(2FBz)_6(H_2O)_4]$.

In this work we present the synthesis and structure of the new dinuclear compound $[Eu_2(\mu_2\text{-}2FBz)_4(2FBz)_2(H\text{-}2FBz)_2(H_2O)_2]$ (**1**) which is isostructural to the previously reported $[Tb_2(\mu_2\text{-}2FBz)_4(2FBz)_2(H\text{-}2FBz)_2(H_2O)_2]$ (**2**) compound[20]. **1** and **2** have been prepared by us from a new straightforward room temperature synthetic method. The coordination number of the lanthanide ions is 9 for **1** and **2.** Suitable single crystals for Single Crystal X-Ray Diffraction were obtained for compound **1**. The obtained powders of **1** and **2** where characterized by infra-red spectroscopy by attenuated total reflectance, elemental analysis, powder X-Ray diffraction and thermogravimetry. Furthermore, for **1** and **2**, the magnetic behaviour and luminescence properties including the emission quantum yield in solid and in water and D_2O solutions are reported.

Results and discussion

Syntheses

In our experiment, we have used a straightforward room temperature synthetic procedure different from the refluxing procedure used to prepare the already published complexes $[Tb_2(\mu_2\text{-}2FBz)_4(2FBz)_2(H\text{-}2FBz)_2(H_2O)_2]$[20] or $[Tb_2(\mu_2\text{-}2FBz)_4(2FBz)_2(H\text{-}2FBz)_2(H_2O)_2]$[21]. We have successfully obtained with our new synthetic procedure the new dinuclear europium(III) compound $[Eu_2(\mu_2\text{-}2FBz)_4(2FBz)_2(H\text{-}2FBz)_2(H_2O)_2]$ (**1**) and the yet structurally published $[Tb_2(\mu_2\text{-}2FBz)_4(2FBz)_2(H\text{-}2FBz)_2(H_2O)_2]$ (**2**). The key of our straightforward room temperature synthetic method is the addition of a big excess of 2-fluorobenzoic acid which occupies two coordination water positions with respect to the previously reported $[Ln_2(2FBz)_6(H_2O)_4]$.

Infrared Spectra

The characteristic bands observed for 2-fluorobenzoic acid (H-2FBz) molecule and compounds **1** and **2** are summarized in *Table 1*. For the Eu(III) and Tb(III) compounds, the characteristic $\nu_{C=O}$ stretching vibration at 1684 cm^{-1} from the free ligand, H-2FBz, disappear in the IR spectra while the asymmetric ($\nu_{as(COO\text{-})}$) and symmetric ($\nu_{s(COO\text{-})}$) absorption peaks of the COO^- group around 1602-104 and 1383-1381 cm^{-1} respectively appear indicating the coordination of the ligands to the lanthanide ions by the oxygen donor atoms. Furthermore, the broad band corresponding to the $\nu_{O\text{-}H}$ of compounds **1** and **2** is different from the band corresponding to the $\nu_{O\text{-}H}$ stretching of the free ligand. The free ligand O-H stretching mainly arises from the COOH group while in the

complexes this vibration is assigned to the H_2O molecules that are coordinated to the Ln^{3+} atoms.

	$\nu_{C=O}$	ν_{H-O}	$\nu_{as(COO^-)}$	$\nu_{s(COO^-)}$
H-2FBz	1685	2870	-	-
1 (Eu)	-	3428	1588	1394
2 (Tb)	-	3419	1602	1383

Table 1. Assignment of selected IR spectra bands for the free ligand and the complexes (cm^{-1})

X-ray Crystal Structure

Structural motif of $[Eu_2(\mu_2\text{-}2FBz)_4(2FBz)_2(H\text{-}2FBz)_2(H_2O)_2]$ 1

Compound **1** crystallizes in a triclinic crystal system with a P-1 space group. A partially labelled molecular plot and the coordination geometry figure is shown in Figure 1. The crystallographic data and selected bond lengths and angles are listed in *Tables S1* and *S2*, respectively.

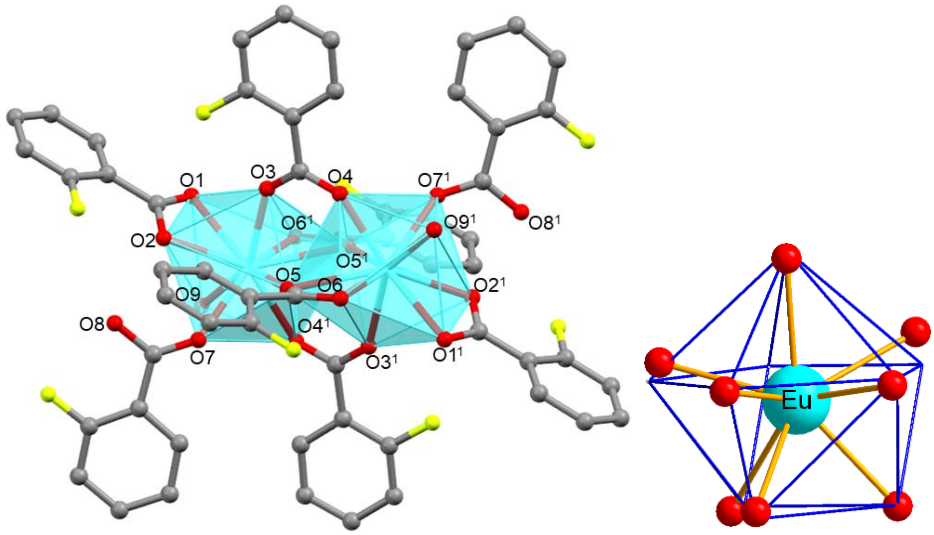

Figure 1. a) Partially labelled plot of compound **1**. H atoms are omitted for clarity. The symmetry transformation used to generate equivalent atoms is [1]: -x+1,-y+1,-z+2. Colour code: grey = C, red = oxygen, green = fluorine and blue = Eu. b) Coordination polyhedron of the Eu(III) ions in compound **1**. The blue line shows the ideal Muffin (MFF-9) polyhedron.

The calculation of the distortion degree of the EuO_9 coordination polyhedron for **1** (Fig. 1b) with respect to ideal nine-vertex polyhedra, using the continuous shape measure theory and SHAPE software,[22,23] shows intermediate distortion between various coordination polyhedra. The lowest continuous shape measures (CShM's) values for compound **1** correspond to Muffin (MFF-9, C_s), Spherical capped square antiprism (CSAPR-9, C_{4v}) and Spherical tricapped trigonal prims (TCTPR-9, D_3h) with values of 1.233, 1.475, 1.999 and 2.617 respectively Fig1b.

The crystal structure of **2** was previously published by Xia Li *et al.*[20] Powder X-ray diffraction measurements (*Figure S1*) have been realized for both synthetized compounds (**1** and **2**) confirming that they are isostructural and that all the product obtained from the reactions is the desired with formula $[Tb_2(\mu_2\text{-}2FBz)_4(2FBz)_2(H\text{-}2FBz)_2(H_2O)_2]$. The calculation of the degree of distortion of the TbO_9 coordination polyhedron for **2** (Fig. 2) with respect to ideal nine-vertex polyhedra, using the continuous shape measure theory and SHAPE software,[22,23] shows intermediate distortion between various coordination polyhedra. The lowest continuous shape measures (CShM's) values for compound **2** correspond to Spherical capped square antiprism (CSAPR-9, C_{4v}), Spherical tricapped trigonal prism (TCTPR-9, D_{3h}) and Tricapped trigonal prism (JTCTPR-9, D_{3h}) with values of 2.337, 2.820 and 2.926 respectively.

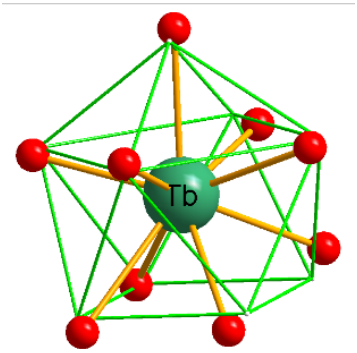

Figure 2. Coordination polyhedron of the Tb(III) ions in compound **2**. The green line shows the ideal Spherical capped square antiprism (CSAPR-9) polyhedron.

The coordination sphere of each Eu(III) is formed by O1 and O2 from a 2FBz ligand in the bidentate chelating coordination mode (Fig.3a) and O7 from an H-2FBz (Fig.3d).

There are two ligands in the bidentate bridging coordination mode (Fig.3b) that are bonded to the Eu(III) atoms through O3 and O4_a and two 2FBz ligands that are in the bidentate chelating bridging coordination mode (Fig.3c) bonded to the lanthanide atom through the O5, O6_a and O5_a atoms. The latest O atom is doubly bridging both Eu(III) centres of the structure. The symmetry transformation used to generate equivalent atoms is _a: -x+1,-y+1,-z+2. Finally, the coordination sphere is completed by O9 from an H_2O molecule. The Eu-O bond length are in the range of 2.348(2) to 2.638(2) Å, the Eu---Eu intramolecular distance is 3.964(3) Å and the O1-Eu-O2 bite angle of the 2FBz ligand in the bidentate chelating coordination mode is 51.69(4)°.

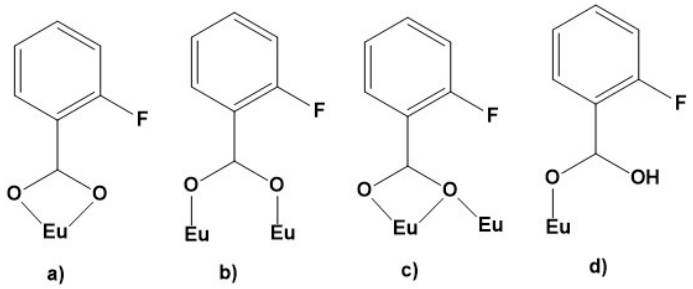

Figure 3. Representation of the different coordination modes of 2-FBz and H-2-FBz ligand. a) chelating bridge b) *syn-syn* bridge c) chelating-bridging d) monodentate for the H-2-FBz acid.

Intermolecular interactions to consider are the O-H---O H-bond from the H_2O molecule and O1 and O6 of two carboxylate groups in the bidentate chelating and bidentate chelating bridging coordination mode respectively. The H9OA/H9OB---O1/O6 distance is 2.020 Å and the O9-H9OA---O1 and O9-H9OB---O6 angles are 154.06° and 149.34°. This arrangement propagates along the [100] direction of the crystal lattice, thus the final supramolecular structure consists of a 1D chain Fig.4.

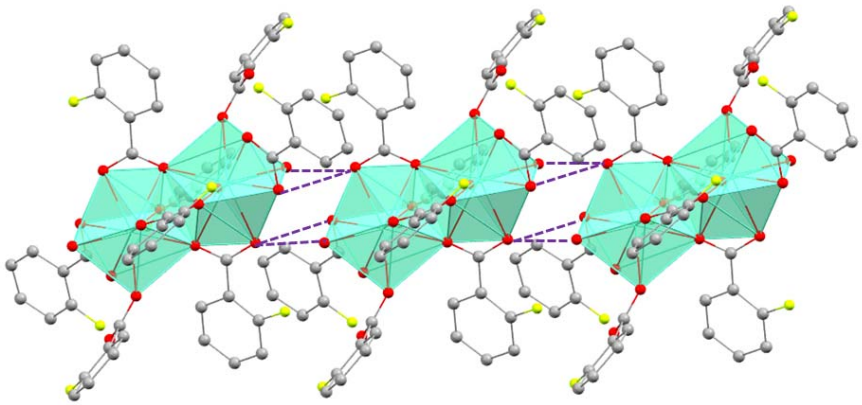

Figure 4. Supramolecular arrangement representation of compound **1** in the [100] direction. In blue: H-O---H intermolecular hydrogen bonds.

Thermal stability

Compounds **1** and **2** are thermally stable until 100 ºC. From this temperature and in the interval 100-250 ºC, **1** and **2** lose the two H-2FBz and the two water molecules: found 21,79% (21,73% expected for **1**); found 21,48 (21,63 % expected for **2**). *Figures S2a* and *S2b* for **1** and **2** respectively.

Photophysical properties of 1 and 2

Photoluminescent properties have been studied in solid state at room temperature for both lanthanide compounds. As stated before, highly luminescent lanthanide(III) coordination compounds can be potentially used as bio-probes. For that, it is important to study the solubility in aqueous solution. For compounds **1** and **2** the solubility values in deionized water were 7.98 and 6.2 mmol/L respectively. Furthermore, photophysical measurements were performed in H_2O and in D_2O solutions at their respective solubility concentrations, in order to study the possible structural changes and the optical properties of **1** and **2** in these media.

Europium compound. Excitation spectra collected at the maximum emission wavelength (λ_{em}) of 617 nm ($^5D_0 \rightarrow {}^7F_2$) showed and intense band at 274 nm for the solid state sample (Eu-s), and at 298 nm for the H_2O (Eu-H_2O) and D_2O (Eu-D_2O) solutions. This band corresponds to the $\pi \rightarrow \pi^*$ transitions centered on the ligand molecules.[17] In addition, for the three excitation spectra, direct *f-f* transitions of Eu(III) could be discerned: $^5D_4 \leftarrow {}^7F_0$ at 361 nm and $^5L_6 \leftarrow {}^7F_0$ at 394 nm, *Figure S3*.

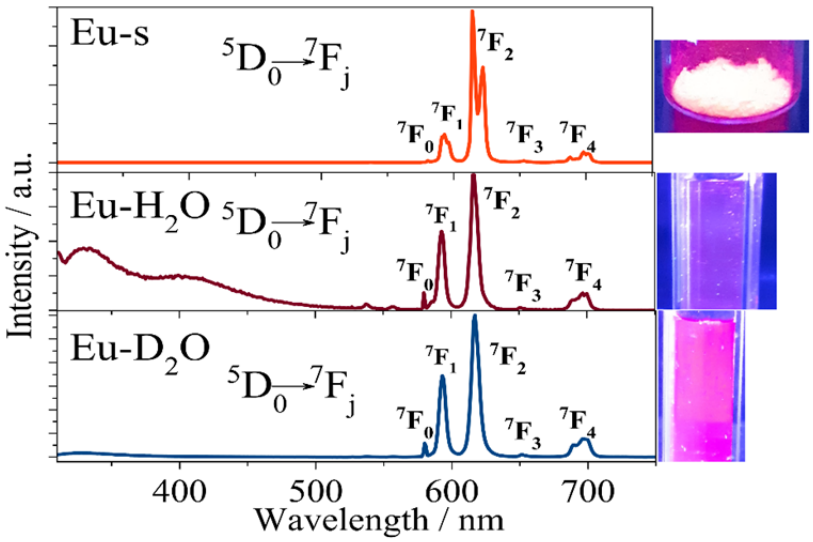

Figure 5. Emission spectra of compound **1** in the microcrystalline sample (Eu-s), dissolved in water (Eu-H_2O) and in deuterium oxide (Eu-D_2O). To the right of the spectra is shown the naked eye luminescence of each sample.

Emission spectra were recorded upon excitation of the samples at the wavelength (λ_{ex}) of 274 nm for the Eu-s sample and at 298 nm for the solution samples Eu-H_2O and Eu-D_2O, that correspond to the ligand absorption maxima. For the three samples, excitation at the ligand wavelength induced the emission of Eu(III), *Figure 5*. The bands that arise from the *f-f* transitions were assigned to $^5D_0 \rightarrow ^7F_0$ at 580 nm, $^5D_0 \rightarrow ^7F_1$ at 593 nm, $^5D_0 \rightarrow ^7F_2$ at 617 nm, $^5D_0 \rightarrow ^7F_3$ at 651 nm and $^5D_0 \rightarrow ^7F_4$ at 698 nm. For the Eu-D_2O and Eu-H_2O samples, residual ligand emission could be seen at the 300-500 nm range, thought for the Eu-D_2O sample, the emission from the lanthanide ion was clearly more intense. For the Eu-s sample, no emission from the ligand was seen, proposing an effective antenna effect. The emission wavelengths of the *f-f* transitions were the same in both the solid sample and the solution samples. Also, the $^5D_0 \rightarrow ^7F_0$ transition appears as a single band for the three samples; therefore, we could assume that the lanthanide ion presents only one type of coordination sphere though high-resolution emission spectra at low temperature measurements are required in order to confirm this statement. Since the degeneracy of the electronic ground state (2J+1) caused by the ligand field effect is one for an Eu(III) ion, any splitting that we can see in the 0 → 0 transition will be due to the presence of compounds with different coordination environment.[24] However, several changes in the band shape and intensity, that are related to a change in the coordination environment of Eu(III) ion, were seen when

dissolving the compounds into aqueous solutions. The $^5D_0 \rightarrow {}^7F_2$ hypersensitive band is the responsible for the red emission of europium and it is sensible to the Eu(III) surroundings. The red emission colour can be seen in the naked eye for the three europium samples, *Figure 5 (right)*. For the Eu-s sample**,** this band is split, meaning that the lanthanide cation is not placed in a position with inversion symmetry inside the structure, but no splitting is seen for the Eu-H_2O and Eu-D_2O systems. In addition, the intensity ratio of the $^5D_0 \rightarrow {}^7F_2$ and $^5D_0 \rightarrow {}^7F_1$ transitions (0→2/0→1 ratio) gives us information about the symmetry of the coordination environment and hence an increasing of this ratio is attributed to an increasing of the asymmetry around the Eu(III) surroundings.[25,26] For **1** the 0→2/0→1 ratio is 5 in the solid state and 2 in water and deuterated oxide solutions respectively, indicating higher symmetry around the Eu(III) ions in the solution samples. This fact indicates a significant change in the coordination environment of the lanthanide anion and therefore a structural change of the $[Eu_2(\mu_2\text{-}2FBz)_4(2FBz)_2(H\text{-}2FBz)_2(H_2O)_2]$ arrangement when the microcrystalline sample is dissolved in water solution. The suggested structural changes account for the solvation of the lanthanide ions and in order to know how many H_2O molecules coordinate to the Eu(III) center, photoluminescence lifetimes (τ_{obs}) in H_2O and D_2O solution were performed *Figure S4*. The emission decays, monitored at a λ_{em} of 617 nm, were fitted monoexponentially ($I(t) = I_0 \exp(-t/\tau_{obs})$) confirming the presence of single emitting species, and the τ_{obs} values were 0.14 ms for the Eu-H_2O sample and 2.68 ms for the Eu-D_2O. The number of the H_2O (q) molecules in the first coordination sphere were calculated using the equation presented by Horrocks and Sudnick (*Equation 1*)[27]:

$$q = A\left(\frac{1}{\tau_{obs(H2O)}} - \frac{1}{\tau_{obs(D2O)}}\right) \qquad \textit{Eq.1}$$

Where $\tau_{obs(H2O)}$ and $\tau_{obs(D2O)}$ are the lifetimes in ms of Eu(III) dissolved in H_2O and D_2O respectively and A is 1.05 for Eu(III). With this equation, q was 7.1.

Using the revised equation presented by Supkowski and Horrocks[28] (*Equation 2*), which also takes into account the H_2O molecules in the second coordination sphere, the q value was also 7.1. B is 0.06 for Eu(III)

$$q = A\left(\frac{1}{\tau_{obs(H2O)}} - \frac{1}{\tau_{obs(D2O)}} - B\right) \qquad \textit{Eq.2}$$

Thus, the europium compound when solved in water solvates to 7 H_2O molecules, probably breaking the dinuclear system, leading to mononuclear europium species with water and 2-fluorobenzoate ligands coordinated to the metal.

In order to study more about the luminescence and sensitization efficiency of both europium solid and aqueous systems, overall quantum yields (QY) were measured and the corresponding photophysical parameters were calculated, *Table 2*. The QY can be defined as the result of multiplying the intrinsic quantum yield (ϕ_{Ln}) by the sensitization efficiency (η_{sens}) as follows in *Equation 3*:

$$QY = \eta_{sens} \cdot \phi_{Ln} \qquad Eq.3$$

The ϕ_{Ln} describes the efficiency of direct absorption and emission of lanthanide *f-f* transitions and η_{sens} indicates the ligand to lanthanide energy transfer efficiency. In addition, the intrinsic quantum yield can be calculated by *Equation 4*:

$$\phi_{Ln} = \frac{\tau_{obs}}{\tau_{rad}} \qquad Eq.4$$

where τ_{rad} refers to the radiative lifetime which corresponds to the lifetime in absence of non-radiative deactivations. Because of pure magnetic dipole character of the $^5D_0 \rightarrow {}^7F_1$ transition, this band is almost independent of local symmetry around Eu(III). Therefore, the τ_{rad} parameter can be calculated from the corrected emission spectrum of the europium compound by means of the *Equation 5*[24,29,30]

$$\frac{1}{\tau_{rad}} = A_{MD,0} \cdot n^3 \left(\frac{I_{TOT}}{I_{MD}}\right) \qquad Eq.5$$

Where $A_{MD,0}$ is a constant (14.65 cm^{-1}), n is the refractive index (1.517 for microcrystalline sample and 1.334 for water) and $\frac{I_{TOT}}{I_{MD}}$ is the ratio between the total integrated area measured from the corrected Eu(III) emission spectrum (I_{TOT}) to the integrated area of the pure magnetic dipole transition $^5D_0 \rightarrow {}^7F_1$ (I_{MD}).[31]

Upon the λ_{ex} of 274 nm, the QY for the polycrystalline sample (Eu-s) was 27%. Also the photoluminescence decay time could be fitted monoexponentially for the solid sample leading to a τ_{obs} value of 0.72 ms. The ϕ_{Ln} and η_{sens} values were 28% and 96% respectively, indicating a very good sensitization efficiency of the europium compound in the solid sample. The values of QY and τ_{obs} for Eu-s are significantly larger than the previous published for the $[Eu_2(2FBz)_6(H_2O)_4]$ compound which are 15% and 0.52 ms

respectively,[17] thus verifying the effect of the highest number of coordinated water molecules in the quantum yield. By dissolving the solid sample of **1** into a 6.2 mmol/L aqueous solution, the QY resulted of 30% for the Eu-D_2O sample and it decreased drastically down to 0.6% for the Eu-H_2O sample. The ϕ_{Ln} and η_{sens} were 2% and 30% respectively for the Eu-H_2O sample.

The lower quantum yield of the Eu-H_2O sample indicates the presence of more favored non-radiative pathways, because of the high energy bond vibrations that are present in the europium ion environment due to the seven inner sphere water molecules. The Eu-D_2O sample yields larger values of ϕ_{Ln} and η_{sens} (34% and 88% respectively). BECAUSE?

	τ_{obs} (ms)	QY (%)	τ_{rad} (ms)	ϕ_{Ln} (%)	η_{sens} (%)
Eu-s	0.72	27	2.58	28	96
Eu-H_2O 7.9 mmol L^{-1}	0.14	0.6	7.48	2	30
Eu-D_2O 7.9 mmol L^{-1}	2.68	30	7.86	34	88

Table 2. Lifetimes (τ_{obs}), Overall Quantum Yields (QY) and the calculated photoluminescence parameters: radiative lifetimes (τ_{rad}), intrinsic quantum yield (ϕ_{Ln}) and sensitization efficiency (η_{sens}) of compound **1** in the microcrystalline sample (Eu-s), dissolved in water (Eu-H_2O) and in deuterium oxide (Eu-D_2O).

Terbium compound. Excitation spectra recorded at the maximum emission wavelength (λ_{em}) of 543 nm for the polycrystalline sample (Tb-s) and at 548 nm ($^5D_4 \rightarrow {}^7F_5$) for the aqueous solutions in H_2O (Tb-H_2O) and D_2O (Tb-D_2O) showed an intense band at 290 nm, for Tb-s, and at 297 nm for Tb-H_2O and Tb-D_2O corresponding to the $\pi \rightarrow \pi^*$ excitation transitions from the ligand moieties, *Figure S5*. Emission spectra under the respective ligand excitation wavelength (λ_{ex} = 290 nm for Tb-s and 297 nm for Tb-H_2O and D_2O) gave rise to the characteristic bands from the *f-f* transitions of the Tb(III) ion, *Figure 6*. For the three samples, the first band at 490 nm is assigned to $^5D_4 \rightarrow {}^7F_6$ whereas the most intense band centered at 544 nm for the Tb-s sample and at 546 nm for the Tb-H_2O and Tb-D_2O samples, corresponds to the $^5D_4 \rightarrow {}^7F_5$ transition, responsible for the green emission colour that can be seen in the naked eye under excitation of UV light for the three different samples of compound **2** (*Figure 6, right).*

Furthermore, the weaker intense bands at 586 and 622 nm were assigned to $^5D_4 \rightarrow {}^7F_4$ and $^5D_4 \rightarrow {}^7F_3$ transitions, respectively.[32]

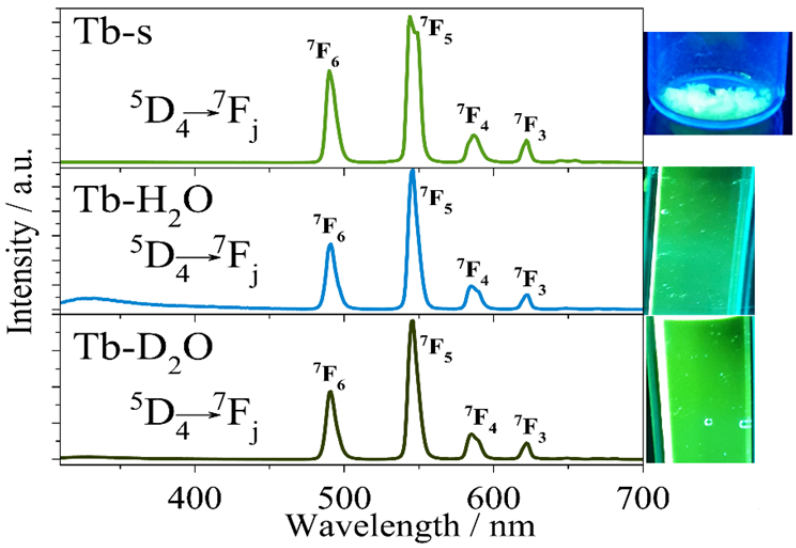

Figure 6. Emission spectra of compound **2** in the microcrystalline sample (Tb-s) and dissolved in water solution (Tb-H_2O) and in deuterium oxide (Tb-D_2O). To the right of the spectra is shown the naked eye luminescence of each sample.

Compilation of the measured photoluminescent parameters of compound **2** are presented in *Table 3*. The measured lifetime for the Tb-H_2O sample was also in the millisecond range (0.50 ms), higher than the τ_{obs} observed for the Eu-H_2O compound (0.14 ms). Compound **2** dissolved in D_2O (Tb-D_2O) reached a τ_{obs} of 1.86 ms. The outcome number of coordination water molecules, q, for the terbium compound was 6.1 taking into account the first coordination sphere (*Equation 1*)[27] and 7 with the developed equation that considers also the second coordination sphere contribution, (*Equation 2*)[33]. The Tb(III) ion coordinates to 5 more molecules of H_2O when dissolved in aqueous solution, shifting 2 nm to the red range the $^5D_4 \rightarrow {}^7F_5$ emission transition. Therefore, structural changes also take place when dissolving the Tb(III) polycrystalline sample in H_2O solution. The QY in solution for compound **2** was 4% (Tb-H_2O) and 26% (Tb-D_2O). Furthermore, for the Tb(III) solid sample the τ_{obs} was 1.43 ms and the compound showed a rather high sensitization quantum yield of 76%. The decay times recorded for the three Tb(III) samples where fitted monoexponentially in agreement with a single emitting species, *Figure S6*

.

	τ_{obs} (ms)	QY (%)
Tb-s	1.43	76
Tb-H_2O 6.2 mmol/L	0.50	4
Tb-D_2O 6.2 mmol/L	1.86	26

Table 3. Lifetimes (τ_{obs}) and Overall Quantum Yields (QY) of compound **2** in the microcrystalline sample (Tb-s), dissolved in water (Tb-H_2O) and in deuterium oxide (Tb-D_2O).

All in all, the emission and sensitization efficiency decreases considerably when the compounds **1** and **2** are dissolved in water because of the luminescence quenching produced by the high O-H vibrators bonds from the water molecules that promote energy loss by non-radiative processes.[1,3] However, the photoluminescence properties still present in water solution taking into account that their luminescence can be seen in the naked eye for compounds **1** and **2**, making them a choice for candidates for bioanalytical applications.

Magnetic properties

Direct current (dc) magnetic susceptibility and magnetization measurements were performed for compounds **1** and **2** on polycrystalline samples. $\chi_M T$ in front of temperature plots in the 2-300 K temperature range under a dc magnetic field of 0.3 T are depicted in Fig.7. At room temperature (300K) the $\chi_M T$ values are 2.8 and 24.3 $cm^3mol^{-1}K$ for **1** and **2** respectively. For **2,** the room temperature $\chi_M T$ value is close to the one expected for two isolated Tb(III) ions at the ground state ($^7F_6$, S=3, L=3, J=6, g_J=3/2) which is 23.64 $cm^3mol^{-1}K$.[1] However, for **1** the room temperature $\chi_M T$ value is not 0, revealing the presence of populated excited J states ($^7F_1$) that are very close in energy to the ground state ($^7F_0$, S=3, L=3, J=0, g_J=0). On cooling the samples, for **1**, $\chi_M T$ values decrease gradually up to 0.03 $cm^3mol^{-1}K$. This value is very close to 0 and it

suggests that the ground state at this temperature (2 K) agrees with m_j=0. The susceptibility values of compound **2** are almost independent in front of temperature until ~50K where they decrease suddenly to a finite value of 12.1 $cm^3mol^{-1}K$. This fact may be attributed to m_j states (split levels form the crystal field) depopulation in the ground state.

Magnetization dependence on applied magnetic field measured at 2 K, *Figure S7*, reveals no saturation at high magnetic fields (5T) with a magnetization value of 0.10 $N\mu_B$ for **1.** Compound **2** at a high applied magnetic field presents a magnetization saturation value of 10.2 $N\mu_B$.

The χ_M versus T plot (Inset Fig.7) for **1** shows a smooth increase of χ_M values. Below 125K, χ_M reach a constant value of 0.012 $cm^3mol^{-1}K$ affirming the thermal depopulation of the mixed $^7F_1$ excited state, and only the $^7F_0$ ground state is populated at this point. At very low temperatures ~4K, the europium compound shows a small increase of χ_M values because of the presence of some remnant paramagnetic species. For an europium ion, the energy difference between the ground state term ($^7F_0$) with the first ($^7F_1$) and second ($^7F_2$) excited levels is small and mixing of these *J* levels can occur because of the crystal field effect or Zeeman effect. The χ_M versus T plot for **2** results in a typical paramagnetic behavior.

The plot of $1/\chi_M$ in front of T resulted in a linear tendency for compound **2** (Fig.8), in the whole measured temperature range, confirming that the terbium compound obeys the Curie Weiss law ($\chi_M = \frac{C}{T-\theta}$). The Curie constant (C) and Weiss temperature (θ) were determined to be 24.2 cm^3mol^{-1} and 2.6 K respectively.

The obtained magnetic results of **1** and **2** are in agreement with other Eu(III) and Tb(III) compounds.[1,32,34-38]

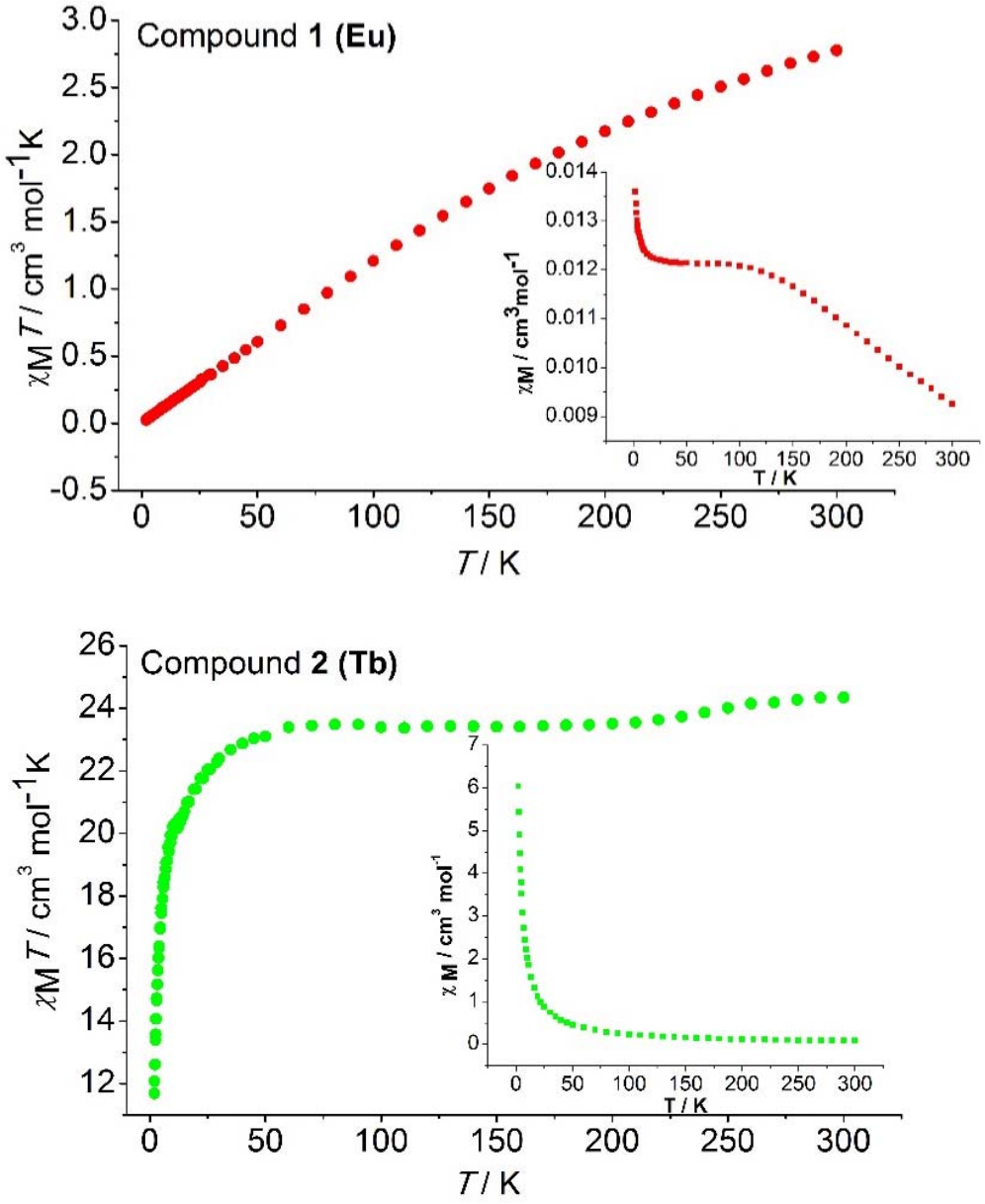

Figure 7. χ_MT vs. *T* plots for compounds **1** and **2**.

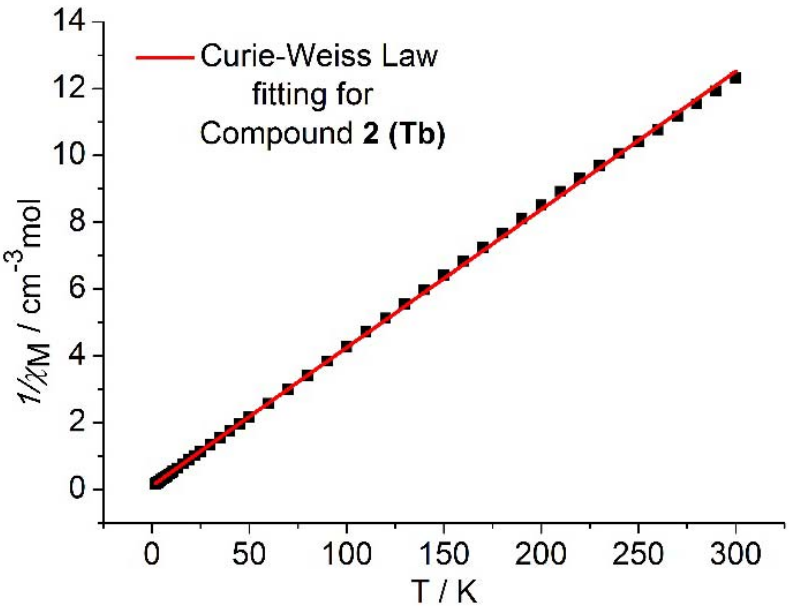

Figure 8. $1/\chi_M$ vs. *T* plot for compound **2**

Conclusions

With the aim to study the effects in the reduction of the number of water molecules in the photoluminescence properties with respect to the previously published compounds of formula $[Ln_2(2FBz)_6(H_2O)_4]$, we have presented the structural, magnetic and luminescence studies of two homodinuclear lanthanide compounds of formula $[Ln_2(\mu_2\text{-}2FBz)_4(2FBz)_2(H\text{-}2FBz)_2(H_2O)_2]$ Ln = Eu (**1**) and Tb (**2**), which show a diminution of the half in the number of coordinated water molecules. From the synthetic point of view, we have used a new straightforward room temperature synthetic procedure to avoid the refluxing step used to prepare the previously published $[Tb_2(\mu_2\text{-}2FBz)_4(2FBz)_2(H\text{-}2FBz)_2(H_2O)_2]$ compound.

The solid-state photoluminescence study of the complexes **1** and **2** shows the 4*f*-4*f* lanthanide transitions in the visible range. The overall quantum yield has values of 27 and 76% for **1** and **2** respectively. For the previously published compounds of formula $[Ln_2(2FBz)_6(H_2O)_4]$ the quantum yields were 15 and 50% for the corresponding Eu and Tb derivatives respectively.[17] Compounds **1** and **2** are water soluble, with solubility values of 7.98 and 6.2 mmol/L for **1** and **2** respectively. The QY decreases to 0.23% and 3.8% for **1** and **2** respectively when dissolved in water. Photoluminescence lifetimes are 0.13 and 0.42 ms for **1** and **2** respectively. In addition, radiative lifetime, intrinsic quantum yield and sensitization efficiency for **1** in water solution are 7.48 ms, 2% and

30% respectively. In **1** and **2** the photoluminescence properties are still present in water solution, making them a choice for candidates for bioanalytical applications.

The magnetic study of **1** and **2** shows no SMM's behavior and is in agreement with other Eu(III) and Tb(III) compounds. [1,32,34-38]

Experimental section

Starting Materials

$Ln(NO_3)_3 \cdot xH_2O$ salts (Strem Chemicals) and 2-Fluorobenzoic acid (Aldrich) were used as received.

Spectral and Magnetic Measurements

The elemental analyses of the compounds were performed at the Serveis Científics i Tecnològics of the Universitat de Barcelona. Infrared spectra (4000-400 cm^{-1}) were recorded from KBr pellets on a Perkin-Elmer 380-B spectrophotometer. Solid state fluorescence spectra were recorded on a Horiba Jobin Yvon SPEX Nanolog fluorescence spectrophotometer at room temperature. Lifetimes were recorded on a DeltaPro TCSPC equipment from Horiba Scientific upon excitation the samples with a 283 nm nanoLED. Luminescent quantum yields were recorded using an Absolute PL quantum yield spectrometer from Hamamatsu Photonics upon excitation the samples at 274 and 290 nm for **1** and **2** respectively.

Thermal analyses were carried out on a thermoanalyzer STA 409 PC Luxx (NETZSCH, Germany) in the temperature range of 30–600 ºC under N_2 atmosphere, with a heating rate of 10 ºC min^{-1}.

Magnetic measurements were performed on solid polycrystalline samples in a Quantum Design MPMS-XL SQUID magnetometer at the Magnetic Measurements Unit of the Universitat de Barcelona. Pascal's constants were used to estimate the diamagnetic corrections, which were subtracted from the experimental susceptibilities to give the corrected molar magnetic susceptibilities.

Solubility

Water solubility of **1** and **2** was measured by refluxing for 1h a suspension of 150 mg of the respective lanthanide compound in 5 mL of deionized water. Then the mixture was let to cool at room temperature. After that, 3 mL of clear solution was putted in a crystallizer of known mass and let it evaporate. The variance in mass of the crystallizer corresponds to the product mass that was dissolved in the 3 mL of deionized water.

X-ray crystallography

A colorless prism-like specimen of **1**, approximate dimensions 0.046 mm x 0.055 mm x 0.181 mm, was used for the X-ray crystallographic analysis. The X-ray intensity data were measured on a D8 Venture system equipped with a multilayer monochromator and a Mo microfocus (λ = 0.71073 Å).

The frames were integrated with the Bruker SAINT software package[39] using a narrow-frame algorithm. The integration of the data using a triclinic unit cell yielded a total of 48286 reflections to a maximum θ angle of 30.58° (0.70 Å resolution), of which 8053 were independent (average redundancy 5.996, completeness = 99.4%, Rint = 3.37%, Rsig = 2.32%) and 7500 (93.13%) were greater than 2σ(F2). The final cell constants of a = 9.0953(8) Å, b = 11.3783(10) Å, c = 13.6591(12) Å, α = 110.681(3)°, β = 93.121(3)°, γ = 92.453(3)°, volume = 1317.6(2) Å3, are based upon the refinement of the XYZ-centroids of reflections above 20 σ(I). Data were corrected for absorption effects using the Multi-Scan method (SADABS).[40] The calculated minimum and maximum transmission coefficients (based on crystal size) are 0.6698 and 0.7461.

The structure was solved and refined using the Bruker SHELXTL Software Package,[41] using the space group P -1, with Z = 1 for the formula unit, C56H38Eu2F8O18. The final anisotropic full-matrix least-squares refinement on F2 with 385 variables converged at R1 = 1.99%, for the observed data and wR2 = 4.67% for all data. The goodness-of-fit was 1.104. The largest peak in the final difference electron density synthesis was 0.998 e-/Å3 and the largest hole was -0.754 e-/Å3 with an RMS deviation of 0.097 e-/Å3. On the basis of the final model, the calculated density was 1.833 g/cm3 and F(000), 716 e-.

Molecular plots were obtained with MERCURY program.

Synthesis of the complexes $[Ln_2(2FBz)_4(2FBz)_2(H\text{-}2FBz)_2(H_2O)_2]$

An ethanol solution (20ml) containing $Ln(NO_3)_3 \cdot nH_2O$ (0.9mmol) was added to an ethanol/H_2O (1:1) solution (20 ml) containing 2-fluorobenzoic acid (540.40 mg, 4 mmol) and pyridine (355.95 mg, 4.5 mmol). After the reagents were dissolved, 2-fluorobenzoic acid (270.2 mg, 2 mmol) was added. The solution was stirred for 30 minutes and then left to stand at room temperature. Single crystals suitable for X-Ray diffraction were obtained within two weeks. The crystals were obtained by filtration and washed with ethanol.

$[Eu_2(\mu_2\text{-}2FBz)_4(2FBz)_2(H\text{-}2FBz)_2(H_2O)_2]$: White crystals. Yield (%) 33. IR: 3418(br), 1666(w), 1604(s, split), 1565(m), 1528(m), 1488(w), 1454(m), 1422(m), 1381(s), 1293(m), 1250(w), 1210(m), 1164(w), 873(m) 856(m), 841(m), 808(m), 789(w), 748(s), 693(w), 655(m), 569(m) cm^{-1}. Anal. Calcd (found) for $C_{56}H_{38}Eu_2F_8O_{18}$: C(%) 46.23 (46.07), H(%) 2.63 (2.39).

$[Tb_2(\mu_2\text{-}2FBz)_4(2FBz)_2(H\text{-}2FBz)_2(H_2O)_2]$: white crystals. Yield (%) 55. IR: 3419(br), 1669(w), 1602(s, split), 1562(m), 1529(m), 1483(w), 1446(m), 1423(m), 1383(s), 1293(m), 1247(w), 1234(m), 1157(w), 1131(w), 1097(m), 1031(w), 951(w), 875(m), 855(m), 842(m), 808(m), 789(w), 749(s), 689(w), 649(m), 563(m) cm^{-1}. Anal. Calcd(found) for $C_{56}H_{38}Tb_2F_8O_{18}$: C(%) 45.80 (45.23), H(%) 2.60 (2.50).

Acknowledgments

R. V. and A.T. acknowledge the financial support from Ministerio de Ciencia, Innovación y Universidades (Spain), Project PGC2018-094031-B-100. L. R. and A. L. acknowledge the financial support from Ministerio de Ciencia, Innovación y Universidades (Spain), PID2019-104121GB-I00.

Conflict of Interest: The authors declare no conflicts of interest.

References

1 D. A. Atwood, Ed., *The Rare Earth Elements: Fundamentals and Applications*, John Wiley & Sons Ltd, 2012. (b) A. de Bettencourt-Dias, Ed., *Luminescence of*

Lanthanide Ions in Coordination Compounds and Nanomaterials. John Wiley & Sons Ltd, 2014.

2 E. G. Moore, A P. S. Samuel and K.N. Raymond, *Acc. Chem. Res.*, 2009, **42**, 542-552.

3 J.-C. G. Bünzli, *Coord. Chem. Rev.*, 2015, **19**, 293–294.

4 Z. Xia, Z. Xu, M. Chen, Q- Liu, *Dalton Trans.,* 2016, **45**, 11214-11232 ; (b) J.-C.G. Bünzli, C. Piguet, *Chem. Soc. Rev.*, 2005, **34**, 1048-1077.

5 J.-C.G. Bünzli, *Acc. Chem. Res.,* 2006, **39**, 53-61 ; (b) S. Swavey and R. Swavey, *Coord. Chem. Rev.*, 2009, **253**, 2627-2638.

6 S.V. Eliseeva and J.-C.G. Bünzli, *Chem. Soc. Rev.*, 2010, **39**, 189-227.

7 E. G. Moore, A. P. S. Samuel and K. N. Raymond, *Acc. Chem. Res.*, 2009, **42**, 542-552.

8 C. P. Montgomery, B. S. Murray, E. J. New, R. Pal and D. Parker, *Acc. Chem. Res.*, 2009, **42**, 925-937.

9 S. J. Butler, M. Delbianco, L. Lamarque, B. K. McMahon, E. R. Neil, R. Pal, D. Parker, J. W. Walton and J. M. Zwier, *Dalton Trans.*, 2015, **44**, 4791-4803.

10 E. J. New, D. Parker, D. G. Smith and J. W. Walton, *Curr. Opin. Chem. Biol*. 2010, **14**, 238−246.

11 S. V. Eliseeva and J.-C. G. Bünzli, *Chem. Soc. Rev.,* 2010, **39**, 189−227.

12 A. D'Aléo, L. Ouahab, C. Andraud, F. Pointillart and O. Maury, *Coord. Chem. Rev*. 2012, **256**, 1604−1620.

13 M. Sy, A. Nonat, N. Hildebrandt and L. J. Charbonnière, *Chem. Commun.* 2016, **52**, 5080−5095.

14 G.-Q. Jin, Y. Ning, J.-X. Geng, Z.-F. Jiang, Y. Wang, and J.-L- Zhang, *Inorg. Chem. Front.* 2020, **7**, 289−299.

15 L. Li, X. Zhao, N. Xiao, Y. Wang, Z. Wang, S. Yang, X. Zhou, *Inorganica Chim. Acta* 2015, **426**, 107–112.

16 V. V. Utochnikova, A. S. Kalyakina, N. N. Solodukhin, and A. N. Aslandukov, *Eur. J. Inorg. Chem.* **2019**, 2320–2332

17 A. S. Kalyakina, V. V. Utochnikova, I. S. Bushmarinov, I. M. Le-Deygen, D. Volz, P. Weis, U. Schepers, N. P. Kuzmina and S. Bräse, *Chem. Eur. J.* 2017, **23**, 14944-14953.

18 B. Casanovas, M. Font-Bardía, S. Speed, M. S. El Fallah and R. Vicente. *Eur. J. Inorg. Chem.*, 2018, 1928-1937.

19 B. Casanovas, S. Speed, R. Vicente and M. Font-Bardía. *Polyhedron*, 2019, **173**, 114113.

20 X. Li, Z.-Y. Zhang, Y.-Q. Zou, *Eur. J. Inorg. Chem.*, 2005, 2909-2918.

21 X. Li, Y.-Q. Zou, H.-B. Song, *J. Chem. Cryst*. 2007, **37**, 555-559.

22 S. Alvarez, P. Alemany, D. Casanova, J. Cirera, M. Llunell and D. Avnir, *Chem. Soc. Rev*. 2005, **249**, 1693–1708.

23 J. Cirera and S. Alvarez, *Dalton. Trans*. 2013, **42**, 7002–7008.

24 K. Binnemans, *Coord. Chem. Rev.*, 2015, **295**, 1–45.

25 J. W. de Oliveira Maciel, M. A. Lemes, A. K. Valdo, R. Rabelo, F. Terra Martins, L. J. Queiroz Maia, R. Costa de Santana, F. Lloret, M. Julve and D. Cangussu. *Inorg. Chem.,* 2021, **60**, 6176−6190.

26 L. Zur, *J. Mol. Struct.*, 2013, **1041**, 50–54.

27 W. DeW. H. Jr. and D. R. Sudnick *J. Am. Chem. Soc.* 1979, **101**, 334–340

28 Supkowski, R. M.; Horrocks, W. D. W., Jr. *Inorg. Chim. Acta* 2002, **340**, 44−48.

29 M. H. V. Werts, R. T. F. Jukes, and J. W. Verhoeven, *Phys. Chem. Chem. Phys.*, 2002, **4**, 1542–1548.

30 A. Aebischer, F. Gumy, and J. C. G. Bünzli, *Phys. Chem. Chem. Phys.*, 2009, **11**, 1346–1353.

31 S. Petoud, S. M. Cohen, J.-C. G. Bünzli, and K. N. Raymond, *J. Am. Chem. Soc*. 2003, **125**, 13324–13325

32 A. J. Kanimozhi and V. Alexander, *Dalt. Trans.*, 2017, **46**, 8562–8571.

33 A. Beeby, I. M. Clarkson and R. J. Dickins, *Chem. Soc., Perkin Trans.* 1999, **2**, 493−504.

34 J. Tang and P. Zhang, *Lanthanide Single Molecule Magnets*. New York Dordrecht London: Spring-Verlag Berlin Heidelberg, 2015.

35 B. Barja, P. Aramendia, R. Baggio, M. T. Garland, O. Peña, and M. Perec, *Inorganica Chim. Acta*, 2003, **355**, 183–190.

36 A. Arauzo, A. Lazarescu, S. Shova, E. Bartolomé, R. Cases, J. Luzón, J. Bartolomé and C. *Dalt. Trans.*, 2014, **43**, 12342–12356.

37 J. Legendziewicz, V. Tsaryuk, V. Zolin, E. Lebedeva, M. Borzechowska and M. Karbowiak, *New J. Chem.*, 2001, **25**, 1037–1042.

38 E. Bartolomé, A. Arauzo, J. Luzón, S. Melnic, S. Shova, D. Prodius, I. C. Nlebedim, F. Bartolomé and J. Bartolomé, *Dalt. Trans.*, 2019, **48**, 5022-5034.

39 SAINT Version 7.**68A**, Bruker AXS Inc., 2009.

40 SADABS Version 2008/1, Sheldrick, Bruker AXS Inc.

41 SHELXTL , G. M. Sheldrick, *Acta Cryst*. 2008, **A64**, 112-122.